

The inclusion complexes between $[\text{Zn}(\text{dmit})_2]^{2-}$ anion and cyclodextrins: studied by induced circular dichroism spectra and density functional theory calculations

Qi Wang · Rui He · Xian Cheng · Changsheng Lu

Received: 20 May 2010 / Accepted: 15 July 2010 / Published online: 30 July 2010
© Springer Science+Business Media B.V. 2010

Abstract A series of inclusion complexes between cyclodextrins (α -, β -, HP- β -, and γ -cyclodextrin, HP- β -cyclodextrin = 2-hydroxypropyl- β -cyclodextrin) and $[\text{Zn}(\text{dmit})_2]^{2-}$ anion (dmit = 1,3-dithiole-2-thione-4,5-dithiolate) were investigated by electronic spectra, induced circular dichroism (ICD) spectra, $^1\text{H-NMR}$ spectra, and quantum chemistry calculations. The stoichiometry of inclusion complexes $[\text{Zn}(\text{dmit})_2]^{2-}$ @cyclodextrins in solution was determined by the method of continuous variation. The experimental data showed that inclusion complex $[\text{Zn}(\text{dmit})_2]^{2-}$ @ β -cyclodextrin adopted 1:2 and 1:1 guest-to-host inclusion ratios in solution, and the inclusion constants (K_{inclu}) were computed to be $5.85 \times 10^7 \text{ M}^{-2}$ and $1.63 \times 10^4 \text{ M}^{-1}$, respectively. In the case of $[\text{Zn}(\text{dmit})_2]^{2-}$ @ γ -cyclodextrin, the continuous variation method showed the inclusion complex adopted 1:1 guest-to-host ratio and K_{inclu} was determined to be $3.27 \times 10^4 \text{ M}^{-1}$. Moreover, inclusion complex $[\text{Zn}(\text{dmit})_2]^{2-}$ @HP- β -cyclodextrin showed different inclusion modes in solution as well. Time-dependent density functional theory (TD-DFT) was used to assist assignment of the ICD signals in inclusion complexes $[\text{Zn}(\text{dmit})_2]^{2-}$ @cyclodextrins. The $p \rightarrow \pi^*$ transition of $[\text{Zn}(\text{dmit})_2]^{2-}$ chromophore, which occurred in the cavity of cyclodextrin, was calculated to be perpendicular to C=C double bonds and thus parallel to the

symmetric axis of the host. When subject to the well-known Harata and Kodaka's rule, the TD-DFT calculations coincided very well with the spectroscopic data in elucidation of the $p \rightarrow \pi^*$ transition relevant ICD signals of $[\text{Zn}(\text{dmit})_2]^{2-}$ @cyclodextrins.

Keywords Cyclodextrin · 1,3-Dithiole-2-thione-4,5-dithiolate · $p \rightarrow \pi^*$ transition · Induced circular dichroism · TD-DFT calculation · Inclusion constant

Introduction

Induced circular dichroism (ICD), a sensitive and powerful method to study the host–guest complexation in solution [1, 2], has been frequently utilized to analyze the alignments of achiral chromophoric guests within chiral host molecules. Although many physical and chemical methods, such as UV, IR, NMR, cyclic voltammograms and thermogravimetric analysis, have been well established [3, 4], ICD is particularly useful for the structural analyses of natural α -, β - and γ -cyclodextrins inclusion complexes [5–7] in solution. The information from the solution structures analyses of host–guest complexation contributes to the understanding of molecular recognition phenomena as well as to that of enzyme–substrate interaction or catalysis [8–12].

In our previous study, we explored inclusion complex Na_2mnt @ β -cyclodextrin (mnt = 2-butene-dinitrile-2,3-dimercapto) in solution [13], where the p - π^* transition in Na_2mnt was investigated by means of ICD, in addition to the well studied π - π^* transitions of the aromatic chromophores or the n - π^* transitions of diazirines and azoalkanes systems [14–16]. Similar to the π -electrons conjugated cores of $\text{M}(\text{mnt})_2$ (M = metals), dmit and related ligands have been used as building blocks for organic, organometallic and

Electronic supplementary material The online version of this article (doi:10.1007/s10847-010-9834-0) contains supplementary material, which is available to authorized users.

Q. Wang · R. He · X. Cheng · C. Lu (✉)
State Key Laboratory of Coordination Chemistry, Nanjing
National Laboratory of Microstructures, School of Chemistry
and Chemical Engineering, Nanjing University, Nanjing 210093,
China
e-mail: luchsh@nju.edu.cn

coordination compound conductors and superconductors over the past 20 years [17–19]. And the research of dmit-relevant chemistry has been attracting increasing concentrations. Consequently in this paper, we chose the transition metal coordination anion $[\text{Zn}(\text{dmit})_2]^{2-}$ as the guest and cyclodextrin (α -, β -, γ -cyclodextrin, and HP- β -cyclodextrin) as the host, and explored their host–guest inclusion complexation in solution based on the strong interactions discovered in inclusion complex $\text{Na}_2\text{mnt}@ \beta$ -cyclodextrin. With the aids of ICD spectra and quantum chemistry calculations (time-dependent density Functional theory, TD-DFT), we studied in detail the p - π^* transition of $[\text{Zn}(\text{dmit})_2]^{2-}$ chromophore inside the cyclodextrins cavities. It is found that the p - π^* transition of the chromophoric guest changed subtly with different hosts, which provided a unique tool for the structural assignments of $[\text{Zn}(\text{dmit})_2]^{2-}@$ cyclodextrins systems in solution.

Materials and methods

Physical measurements and materials

The UV spectra were recorded on a Shimadzu UV-3100 spectrometer. The ICD measurements were performed on a JASCO J-810 circular dichroism spectrometer. The path-length of cell used is 1 cm, and all the data recorded were on the average of three measurements. $^1\text{H-NMR}$ spectra were recorded on a Bruker AVANCE-500 spectrometer in a mixed-solvent of 10% (v/v) dimethyl sulfoxide- d_6 ($\text{DMSO-}d_6$) in deuterium-oxide (D_2O) at 15 °C. *N,N*-dimethylformamide (DMF) was distilled under reduced pressure in an N_2 atmosphere before use. All the cyclodextrins were purchased from Seebio Biotechnology Inc. (P. R. China), (HP- β -cyclodextrin has a 70% substitution degree, which is about 5 hydroxyl groups substituted by hydroxypropyl groups per molecule of β -cyclodextrin at its secondary face) and the reagents employed were commercially available and used as received without further purification. $[\text{Zn}(\text{dmit})_2](\text{NEt}_4)_2$ was synthesized according to the method described in literature [20].

Quantum chemistry calculations

TD-DFT methods from the Gaussian 03 package [21] at the RTD-B3LYP-FC level using a 6-31+G(d,p) basis set were utilized to investigate the properties of absorption bands in UV and ICD spectra.

Preparation of the inclusion complexes in solution

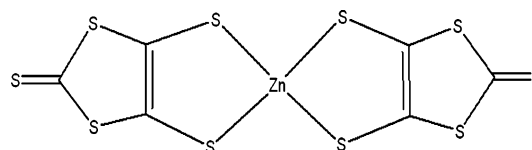
All the inclusion complexes were prepared in solution by similar methods. As $[\text{Zn}(\text{dmit})_2](\text{NEt}_4)_2$ had a poor

solubility in water, the guest compound was dissolved in minimal DMF to achieve 5.0×10^{-5} mol/L aqueous solution. And the $[\text{Zn}(\text{dmit})_2]^{2-}$ aqueous solution was then titrated with increasing concentrations of cyclodextrin solution. $[\beta\text{-cyclodextrin}] = 0, 2.25, 4.5, 9.0, 13.5, 18.0, 22.5, 45.0, 67.5, 90.0, 112.5, 135.0, 157.5, 180.0 \times 10^{-5}$ mol/L; $[\alpha\text{-cyclodextrin}] = 0, 2.5, 5.0, 10.0, 15.0, 20.0, 25.0, 30.0, 35.0, 40.0 \times 10^{-5}$ mol/L; $[\text{HP-}\beta\text{-cyclodextrin}] = 0, 2.5, 5.0, 10.0, 20.0, 25.0, 30.0, 35.0, 40.0 \times 10^{-5}$ mol/L; $[\gamma\text{-cyclodextrin}] = 0, 2.5, 5.0, 10.0, 15.0, 20.0, 25.0, 30.0, 35.0, 40.0 \times 10^{-5}$ mol/L.

Results and discussion

ICD spectra can be a unique tool to directly reflect the angles and positions of included guests inside hosts' cavities. The ICD signals of an achiral guest chromophore could be recordable when it is located in a chiral environment of cyclodextrin cavity. According to the Harata and Kodaka's rule [1, 2], a positive/negative ICD signal arises when the electric transition dipole moment of the chromophore included is aligned parallel/perpendicular to the symmetry axis of cyclodextrin. However, the totally reversed conclusion dominates when the electric transition moment is outside the host cavity. Up to date, it seems that the Harata and Kodaka's rule has been working well in elucidation of the π - π^* transition relevant ICD signals of the aromatic chromophores and the n - π^* transition relevant ICD signals of diazirines and azoalkanes systems [14–16]. By switching to the p - π^* transition of $[\text{Zn}(\text{dmit})_2]^{2-}$ chromophore (Scheme 1), we want to assess the validity of Harata and Kodaka's rule in our conjugated π -systems.

In order to prepare the inclusion complex of $[\text{Zn}(\text{dmit})_2]^{2-}$ with cyclodextrins efficiently, we introduced a small quantity of polar organic solvent (DMF) to dissolve $[\text{Zn}(\text{dmit})_2](\text{NEt}_4)_2$ salt in aqueous solution. Therefore, the guest anion $[\text{Zn}(\text{dmit})_2]^{2-}$ would experience mixed-solvent atmosphere during its complexation with the host. Since the cation of $[\text{Zn}(\text{dmit})_2](\text{NEt}_4)_2$ is so bulky and transparent under our spectroscopic conditions that it would not penetrate into the hosts' cavities and not interfere with the electronic spectra and ICD signals of inclusion complexes $[\text{Zn}(\text{dmit})_2]^{2-}@$ cyclodextrins.



Scheme 1 The structure of the guest $[\text{Zn}(\text{dmit})_2]^{2-}$ anion

Inclusion complex $[\text{Zn}(\text{dmit})_2]^{2-}$ @ β -cyclodextrin

The un-included guest ($[\text{Zn}(\text{dmit})_2]^{2-}$) presented three visible absorptions at around 468, 304, and 276 nm in its electronic spectra (curve 1, Fig. 1). However, when titrated with increasing concentrations of β -cyclodextrin solutions, the absorption maximum shifted to 518 and 312 nm, respectively (curves 2–14, Fig. 1). In addition, the absorption shoulder at around 276 nm merged gradually with that at around 312 nm. The bathochromic shifts during the titration process indicated the formation of inclusion complex $[\text{Zn}(\text{dmit})_2]^{2-}$ @ β -cyclodextrin in solution. It is ascribed to the microenvironment change of $[\text{Zn}(\text{dmit})_2]^{2-}$ when included by β -cyclodextrin, compared with that of the un-included $[\text{Zn}(\text{dmit})_2]^{2-}$.

In the meantime, the free (un-included) guest showed no ICD signals in solution (curve 1, Fig. 1), due to the highly symmetric structure of $[\text{Zn}(\text{dmit})_2]^{2-}$. However, the bisignate ICD signals were recorded upon complexation of

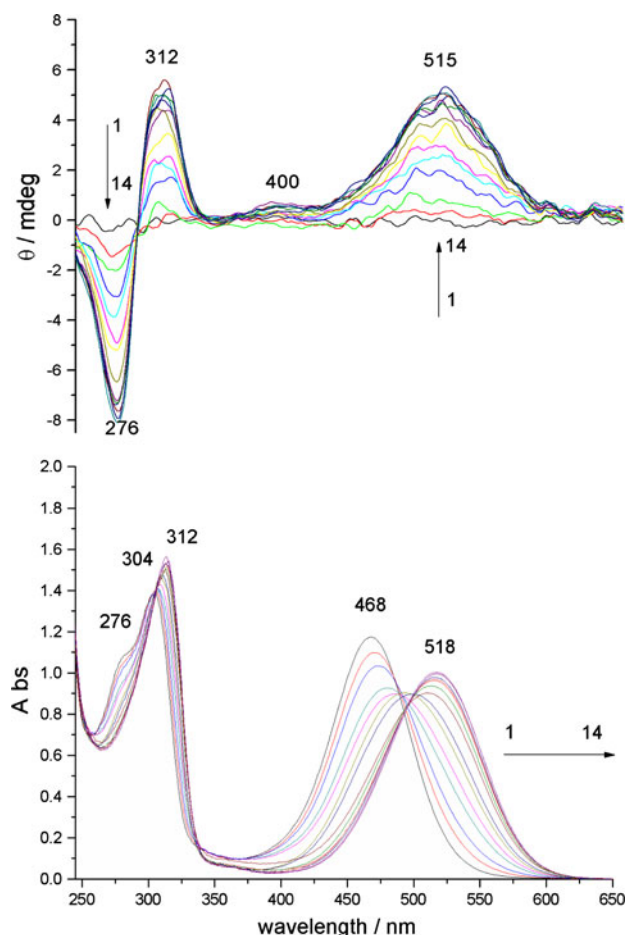


Fig. 1 ICD (above) and UV (below) spectra of $[\text{Zn}(\text{dmit})_2]^{2-}$ ($[\text{Zn}(\text{dmit})_2]^{2-} = 5.0 \times 10^{-5}$ mol/L) in 3% DMF aqueous solution and in the presence of increasing concentrations of β -cyclodextrin; $[\beta\text{-cyclodextrin}] = 0, 2.25, 4.5, 9.0, 13.5, 15.0, 22.5, 45.0, 67.5, 90.0, 112.5, 135.0, 157.5, 180.0 \times 10^{-5}$ mol/L for curves 1–14

$[\text{Zn}(\text{dmit})_2]^{2-}$ with β -cyclodextrin, with one positive peak at around 312 nm and the other negative at around 276 nm. Moreover, one broad positive peak was observed at 515 nm and increased with the addition of β -cyclodextrin solution. It is well known that an achiral guest will be induced by chiral cyclodextrin cavity to produce ICD signals. Accordingly, the formation of inclusion complex $[\text{Zn}(\text{dmit})_2]^{2-}$ @ β -cyclodextrin was confirmed by its ICD spectra.

In order to figure out the solution structure of inclusion complex $[\text{Zn}(\text{dmit})_2]^{2-}$ @ β -cyclodextrin, first of all the stoichiometry of the inclusion complex was determined via the method of continuous variation [13]. Taking into account the over-complicated UV signals of the inclusion complexation (Fig. 1), the stoichiometry and inclusion constant (K_{inclu}) of $[\text{Zn}(\text{dmit})_2]^{2-}$ @ β -cyclodextrin were determined based on the measurements of ICD signals at 515 nm. The Job's plot (continuous variation method) of $[\text{Zn}(\text{dmit})_2]^{2-}$ @ β -cyclodextrin showed that there might be two inclusion modes in solution (Fig. 2). It seemed that at low guest-to-host ratio, the 1:2 (guest:host) inclusion complex tended to dominate, and high guest-to-host ratio produced 1:1 (guest:host) inclusion complex in solution. Therefore, K_{inclu} of inclusion complex $[\text{Zn}(\text{dmit})_2]^{2-}$ @ β -cyclodextrin were computed to be $5.85 \times 10^7 \text{ M}^{-2}$ and $1.63 \times 10^4 \text{ M}^{-1}$ respectively, with the guest-to-host ratio being 1:2 and 1:1 (Fig. 3). Compared with those reported data in literature [22–25], these two inclusion constants suggested strong interaction between the host and the guest.

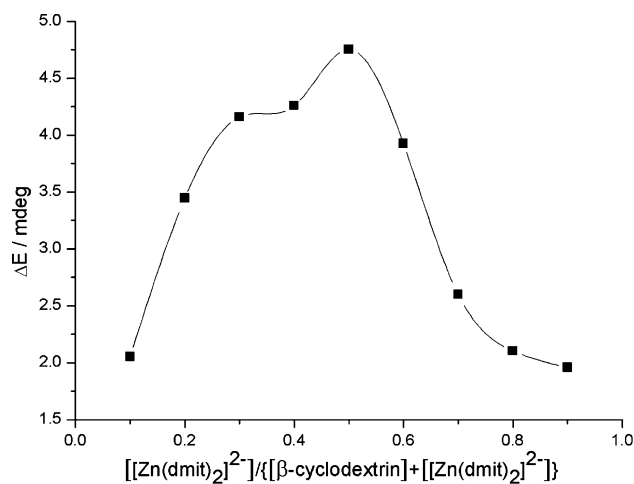


Fig. 2 Continuous variation measurements for inclusion complex $[\text{Zn}(\text{dmit})_2]^{2-}$ @ β -cyclodextrin ($[\text{Zn}(\text{dmit})_2]^{2-} + [\beta\text{-cyclodextrin}] = 1.0 \times 10^{-4}$ mol/L) in 3% DMF aqueous solution at 20 °C (Data is collected at $\lambda = 515$ nm, and ΔE is ICD absorbance of the included guest $[\text{Zn}(\text{dmit})_2]^{2-}$ at the measuring wavelength)

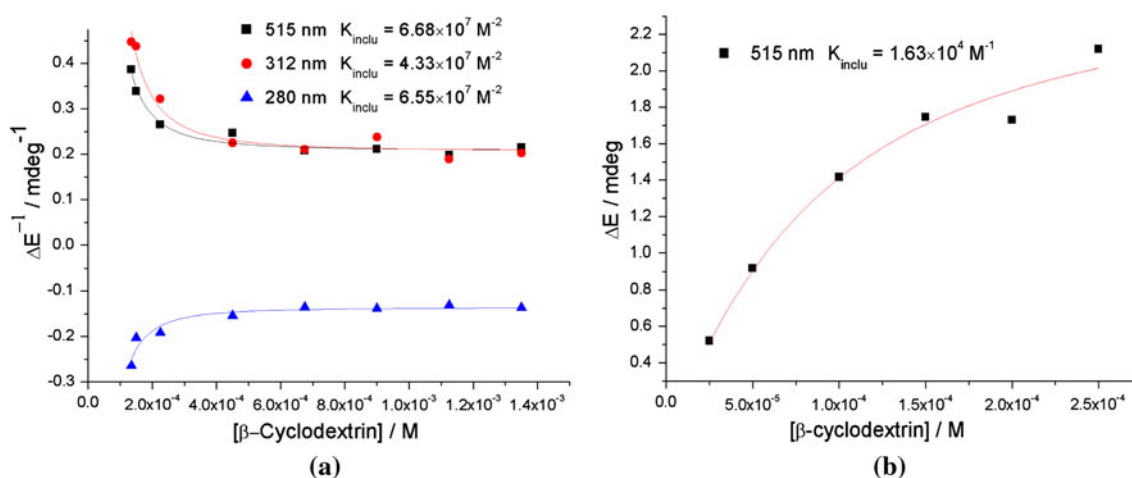


Fig. 3 a Determination of K_{inclu} by using Benesi–Hildebrand fitting method [11], where ΔE^{-1} was plotted versus $[\beta\text{-cyclodextrin}]$ (data collected at around 515, 312, and 280 nm respectively); the stoichiometry of the inclusion complex is 1:2, $K_{\text{inclu}} = 5.85 \times 10^7 \text{ M}^{-2}$;

b Determination of K_{inclu} by using an unilinear fitting method; the stoichiometry of the inclusion complex is 1:1, $K_{\text{inclu}} = 1.63 \times 10^4 \text{ M}^{-1}$

Inclusion complex $[\text{Zn}(\text{dmit})_2]^{2-}$ @ α -cyclodextrin

As shown in Fig. 4, two strong peaks were observed for the free guest ($[\text{Zn}(\text{dmit})_2]^{2-}$) at around 468 and 304 nm, as well as one absorption shoulder at about 276 nm (curve 1). The absorption maximum changed with the increasing concentrations of α -cyclodextrin (curves 2–10). However, no peak-shift took place, which is quite different from that in inclusion complex $[\text{Zn}(\text{dmit})_2]^{2-}$ @ β -cyclodextrin. The dimension of the host might provide an explanation for the minor signal change in that of inclusion complex $[\text{Zn}(\text{dmit})_2]^{2-}$ @ α -cyclodextrin. As the cavity of α -cyclodextrin was too small to include the whole guest, the microenvironment of $[\text{Zn}(\text{dmit})_2]^{2-}$ anion was less influenced. Therefore the UV signal was almost the same as that of the free $[\text{Zn}(\text{dmit})_2]^{2-}$ in solution during the titration of α -cyclodextrin solutions.

Since ICD is more sensitive to explore inclusion complexation, the titration process of $[\text{Zn}(\text{dmit})_2]^{2-}$ with α -cyclodextrin was recorded as well. As showed in Fig. 4, the ICD spectra of the inclusion complex presented two positive peaks at around 304 and 456 nm, and two negative peaks at around 272 and 395 nm. It was somehow strange that the intensities of positive peaks were much stronger than those of the negative ones. The formation of inclusion complex $[\text{Zn}(\text{dmit})_2]^{2-}$ @ α -cyclodextrin was then evidently confirmed by its ICD spectra. Compared with the UV spectra (Fig. 4), the ICD spectra of inclusion complex $[\text{Zn}(\text{dmit})_2]^{2-}$ @ α -cyclodextrin are much more characteristic and sensitive in identifying the host–guest complexation.

Inclusion complex $[\text{Zn}(\text{dmit})_2]^{2-}$ @HP- β -cyclodextrin

Similar to that of inclusion complex $[\text{Zn}(\text{dmit})_2]^{2-}$ @ β -cyclodextrin, the absorption maximum of the guest

molecule shifted from 304 and 468 nm to 322 and 514 nm respectively, with the increasing concentrations of HP- β -cyclodextrin solutions (Fig. 5). At the meantime, the shoulder peak around 276 nm of the un-included guest disappeared. The electronic spectra confirmed the formation of inclusion complex $[\text{Zn}(\text{dmit})_2]^{2-}$ @HP- β -cyclodextrin in solution.

In addition, bisignate ICD signals of the guest during inclusion complexation with HP- β -cyclodextrin were recorded, with one positive peak at around 307 nm and the other negative at around 272 nm. Moreover, one broad positive peak was showed at 514 nm and increased with the addition of HP- β -cyclodextrin solution. As a result, the formation of inclusion complex $[\text{Zn}(\text{dmit})_2]^{2-}$ @HP- β -cyclodextrin was confirmed by its ICD spectra as well.

The Job's plot of $[\text{Zn}(\text{dmit})_2]^{2-}$ @HP- β -cyclodextrin system was unsymmetrical, which was based on the measurements of ICD signals at 514 nm. The result suggested that there were different inclusion modes in solution (Fig. 6), and the maximum at 0.4 strongly accounted for the 2:3 guest-to-host ratio in solution.

Inclusion complex $[\text{Zn}(\text{dmit})_2]^{2-}$ @ γ -cyclodextrin

The absorption maximum of $[\text{Zn}(\text{dmit})_2]^{2-}$ shifted from 468 to 484 nm when titrated with increasing concentrations of γ -cyclodextrin solutions (Fig. 7). The bathochromic effect also indicated the formation of the inclusion complex in solution. The UV spectra showed only one joint, which strongly suggested the single composition of inclusion complex $[\text{Zn}(\text{dmit})_2]^{2-}$ @ γ -cyclodextrin in solution.

However, inclusion complex $[\text{Zn}(\text{dmit})_2]^{2-}$ @ γ -cyclodextrin showed weak ICD signals in solution. The ICD spectra exhibited two positive (294 and 483 nm) and two

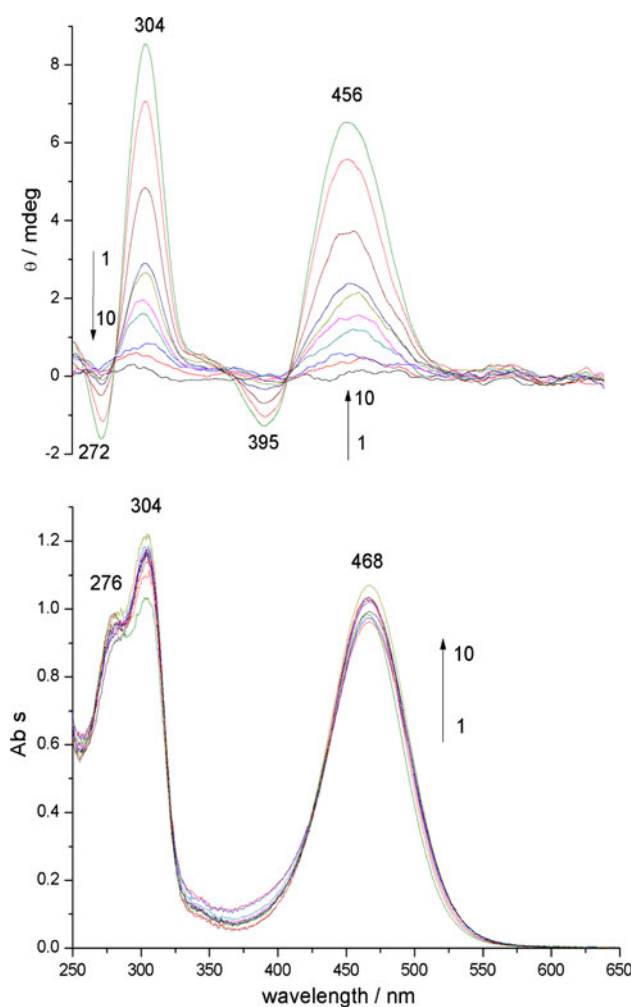


Fig. 4 ICD (above) and UV (below) spectra of $[\text{Zn}(\text{dmit})_2]^{2-}$ ($[\text{Zn}(\text{dmit})_2]^{2-} = 5.0 \times 10^{-5}$ mol/L) in 3% DMF aqueous solution and in the presence of increasing concentrations of α -cyclodextrin; $[\alpha\text{-cyclodextrin}] = 0, 2.5, 5.0, 10.0, 15.0, 20.0, 25.0, 30.0, 35.0, 40.0 \times 10^{-5}$ mol/L for curves 1–10

negative peaks (271 and 400 nm), providing an evidence to confirm the formation of inclusion complex $[\text{Zn}(\text{dmit})_2]^{2-} @ \gamma\text{-cyclodextrin}$. As the cavity of γ -cyclodextrin is larger, we proposed that the guest ($[\text{Zn}(\text{dmit})_2]^{2-}$) included inside the host cavity was too flexible to be able to produce intensive ICD signals [1, 2].

Continuous variation method of $[\text{Zn}(\text{dmit})_2]^{2-} @ \gamma\text{-cyclodextrin}$ system showed that the inclusion complex adopted 1:1 guest-to-host inclusion ratio in solution (Fig. 8). Since the signals collected from ICD spectra were not intensive, the inclusion constants (K_{inclu}) of inclusion complex $[\text{Zn}(\text{dmit})_2]^{2-} @ \gamma\text{-cyclodextrin}$, when computed based on the measurements at different wavelengths, were found to differ from each other. And the average was determined to be $3.27 \times 10^4 \text{ M}^{-1}$ (Fig. 9). However, K_{inclu} of inclusion complex $[\text{Zn}(\text{dmit})_2]^{2-} @ \gamma\text{-cyclodextrin}$ could still set a criterion for $[\text{Zn}(\text{dmit})_2]^{2-} @ \beta\text{-cyclodextrin}$

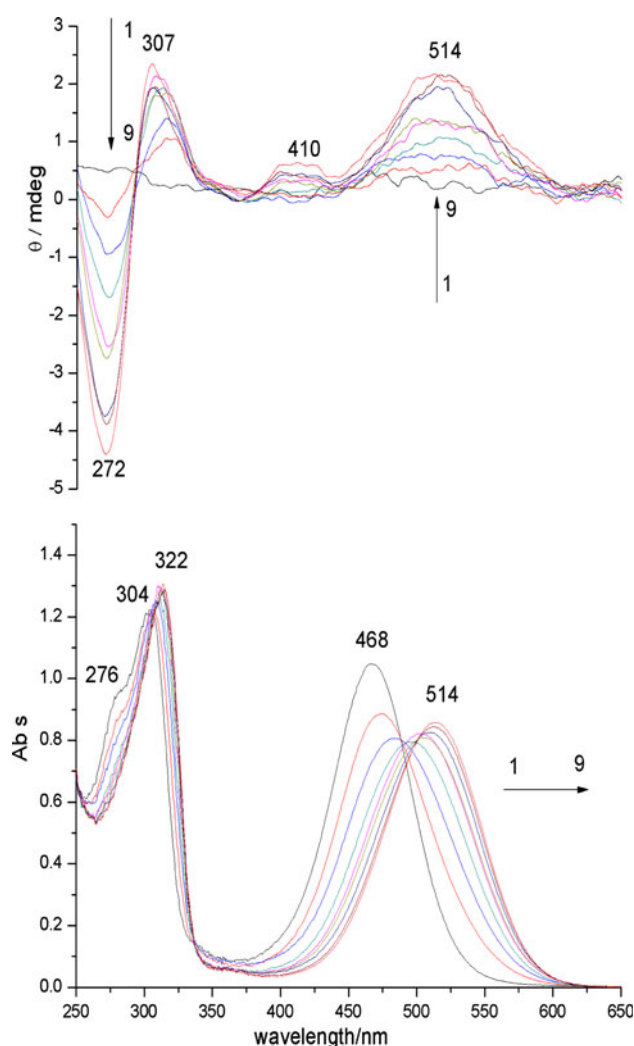


Fig. 5 ICD (above) and UV (below) spectra of $[\text{Zn}(\text{dmit})_2]^{2-}$ ($[\text{Zn}(\text{dmit})_2]^{2-} = 5.0 \times 10^{-5}$ mol/L) in 3% DMF aqueous solution and in the presence of increasing concentrations of HP- β -cyclodextrin; $[\text{HP-}\beta\text{-cyclodextrin}] = 0, 2.5, 5.0, 10.0, 20.0, 25.0, 30.0, 35.0, 40.0 \times 10^{-5}$ mol/L for curves 1–9

system, as the guest-to-host ratio of $[\text{Zn}(\text{dmit})_2]^{2-} @ \gamma\text{-cyclodextrin}$ has been evidently determined to be 1:1. In the case of $[\text{Zn}(\text{dmit})_2]^{2-} @ \beta\text{-cyclodextrin}$, there were two inclusion modes disclosed in solution (Fig. 2). The K_{inclu} of 1:1 ratio inclusion complex was computed to be $1.63 \times 10^4 \text{ M}^{-1}$ based on limited data (vide supra, Fig. 3) by using an unlinear fitting method. Compared with that of inclusion complex $[\text{Zn}(\text{dmit})_2]^{2-} @ \gamma\text{-cyclodextrin}$, the K_{inclu} of $[\text{Zn}(\text{dmit})_2]^{2-} @ \beta\text{-cyclodextrin}$ were credible.

NMR spectra of inclusion complex $[\text{Zn}(\text{dmit})_2]^{2-} @ \beta\text{-cyclodextrin}$

NMR spectroscopy has been used as an important tool for the studies of cyclodextrin inclusion complexes [26]. Since $[\text{Zn}(\text{dmit})_2]^{2-}$ had a poor solubility in water, we prepared

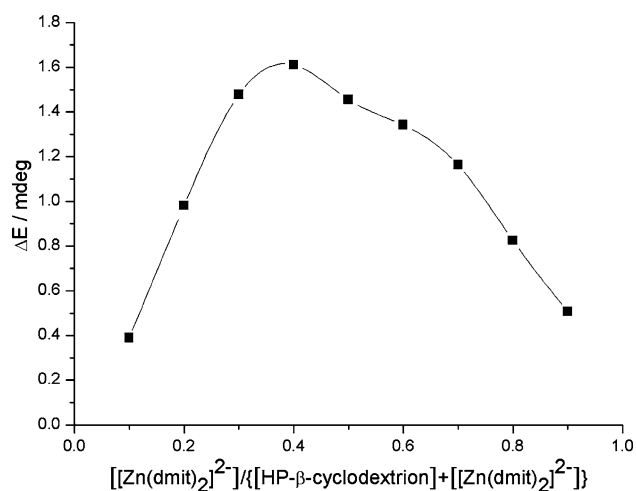


Fig. 6 Continuous variation measurements for inclusion complex $[\text{Zn}(\text{dmit})_2]^{2-}$ @HP- β -cyclodextrin ($[\text{Zn}(\text{dmit})_2]^{2-}$ + [HP- β -cyclodextrin] = 1.0×10^{-4} mol/L) in 3% DMF aqueous solution at 20 °C (data collected at $\lambda = 514$ nm)

the inclusion complexes in a mixed-solvent of D_2O and minimal DMSO-d_6 (up to 10%). Detailed proton signals inspection of β -cyclodextrin in its mixture with $[\text{Zn}(\text{dmit})_2]^{2-}$ was performed and the results displayed most remarkable down-field shifts in the H-5 protons (Fig. 10). Other β -cyclodextrin protons (H-1 and H-2) displayed up-field shifts in the presence of $[\text{Zn}(\text{dmit})_2]^{2-}$. The chemical shifts (δ) changes were not coincident with the previous reports that the H-3 and H-5 protons located inside β -cyclodextrin cavity and were more strongly influenced to produce high-field shifts during the formation of cyclodextrin inclusion complexes [27, 28].

The stoichiometry of inclusion complex $[\text{Zn}(\text{dmit})_2]^{2-}$ @ β -cyclodextrin was also determined by the continuous variation method [29]. As there was no proton on $[\text{Zn}(\text{dmit})_2]^{2-}$, the experimentally observed signals were the δ of β -cyclodextrin protons which were sensitive to inclusion complex formation. The job's plot for the H-5 protons of β -cyclodextrin is presented in Fig. 11. This plot was unsymmetrical and suggested different compositions of inclusion complex $[\text{Zn}(\text{dmit})_2]^{2-}$ @ β -cyclodextrin in solution with 1:1 and 1:2 stoichiometry, respectively. Chemical shifts were reported in ppm and the chemical shifts changes ($\Delta\delta$) were calculated by using the formula: $\Delta\delta = \delta(\text{complex}) - \delta(\text{free})$. The result was consistent with that obtained from ICD measurements (Fig. 2).

TD-DFT calculation results

Since the UV and ICD spectra of inclusion complexes $[\text{Zn}(\text{dmit})_2]^{2-}$ @cyclodextrins were complicated, it was challenging to figure out the assignments of these signals by theoretical methods. As is known, excited states in

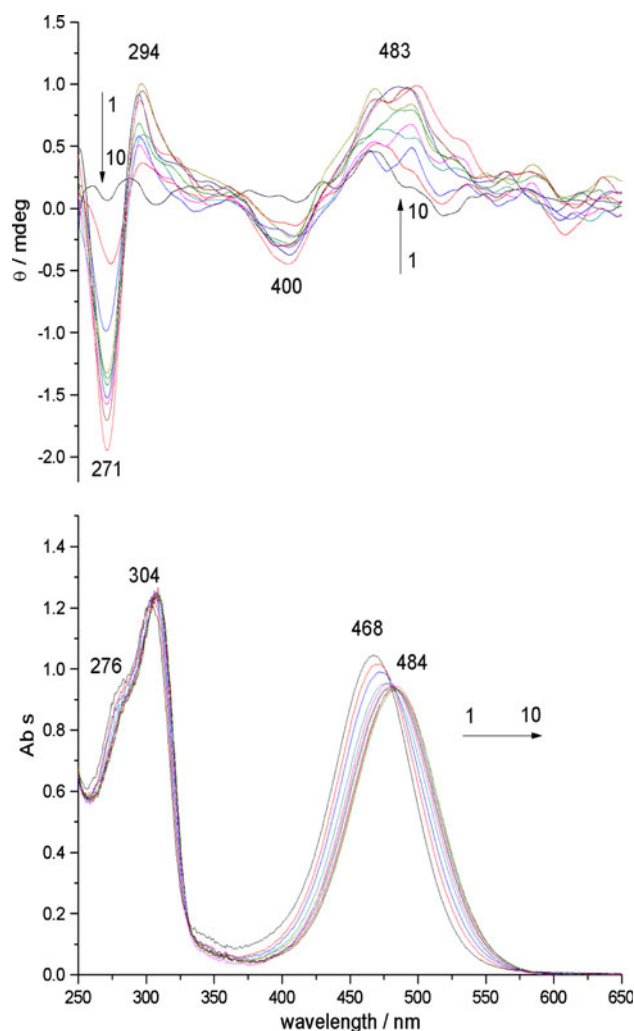


Fig. 7 ICD (above) and UV (below) spectra of $[\text{Zn}(\text{dmit})_2]^{2-}$ ($[\text{Zn}(\text{dmit})_2]^{2-}$ = 5.0×10^{-5} mol/L) in 3% DMF aqueous solution and in the presence of increasing concentrations of γ -cyclodextrin; $[\gamma\text{-cyclodextrin}] = 0, 2.5, 5.0, 10.0, 15.0, 20.0, 25.0, 30.0, 35.0, 40.0 \times 10^{-5}$ mol/L for curves 1–10

general and optical spectra in particular can be predicted from first principles using TD-DFT method [30–32], which has been proven to be a reliable method for studying excited states in broad classes of relatively large systems with good precision [33]. Therefore, we recruited TD-DFT methods from the Gaussian 03 package [21] at the B3LYP level using a 6-31+G(d,p) basis set to investigate the inclusion complexation between $[\text{Zn}(\text{dmit})_2]^{2-}$ and cyclodextrins, and the properties of above-mentioned absorption bands in UV and ICD spectra. However before applying TD-DFT calculations, it is necessary to verify the accessibility of this method in our cases.

In the case of classical inclusion complex *p*-nitrophenol@ β -cyclodextrin (the guest molecule and its computed Cartesian axes were illustrated in Scheme 2), the TD-DFT calculations showed the most intensive absorption of

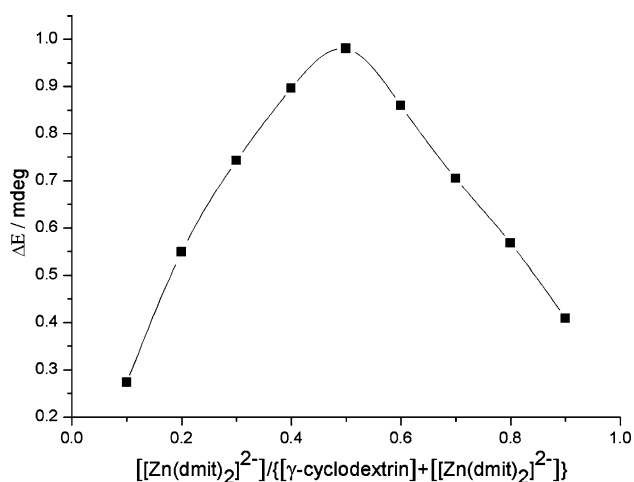


Fig. 8 Continuous variation measurements for inclusion complex $[\text{Zn}(\text{dmit})_2]^{2-}$ @ γ -cyclodextrin ($[\text{Zn}(\text{dmit})_2]^{2-}$ + $[\gamma\text{-cyclodextrin}] = 1.0 \times 10^{-4}$ mol/L) in 3% DMF aqueous solution at 20 °C (data collected at $\lambda = 483$ nm)

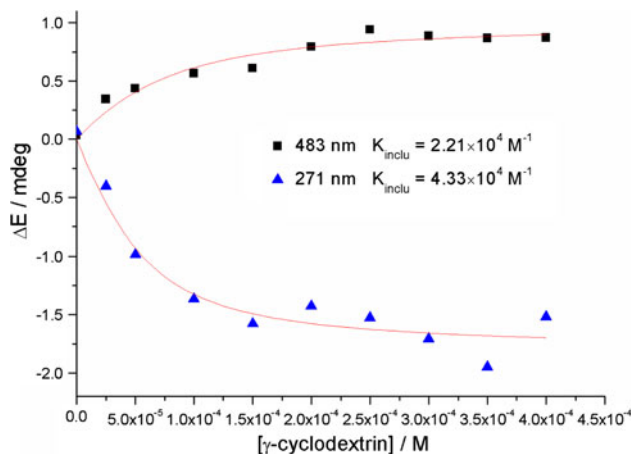


Fig. 9 Determination of K_{inclu} by using an unilinear fitting method, where ΔE was plotted versus $[\gamma\text{-cyclodextrin}]$ (data collected at 483 and 271 nm); the stoichiometry of the inclusion complex is 1:1, $K_{\text{inclu}} = 3.27 \times 10^4 \text{ M}^{-1}$

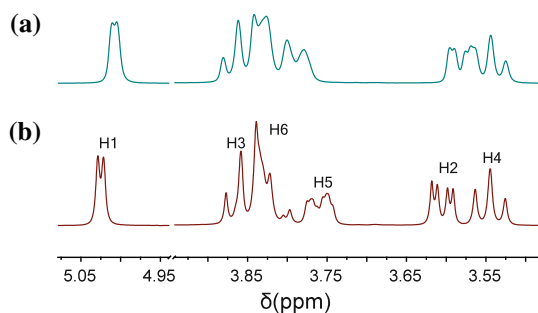


Fig. 10 Partial 500 MHz $^1\text{H-NMR}$ spectra of β -cyclodextrin (in 10% $\text{DMSO-d}_6 - \text{D}_2\text{O}$ solution) in absence (a) and presence of $[\text{Zn}(\text{dmit})_2]^{2-}$ (b)

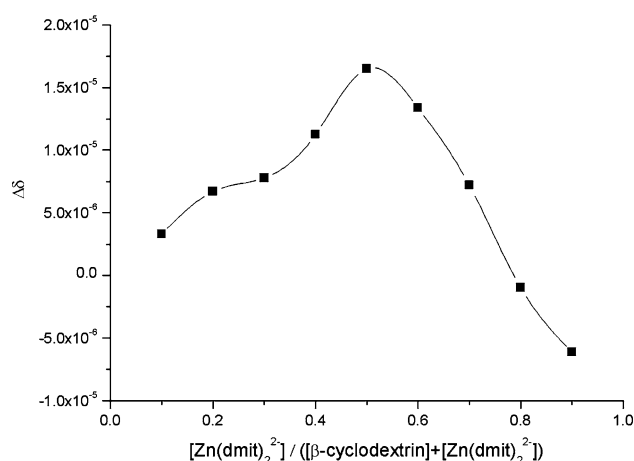
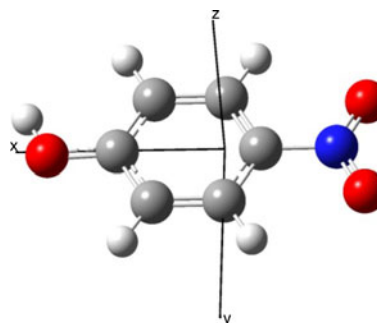


Fig. 11 Continuous variation measurements for inclusion complex $[\text{Zn}(\text{dmit})_2]^{2-}$ @ β -cyclodextrin ($[\text{Zn}(\text{dmit})_2]^{2-}$ + $[\beta\text{-cyclodextrin}] = 1.0 \times 10^{-3}$ mol/L) in 10% $\text{DMSO-d}_6 - \text{D}_2\text{O}$ (data collected from H-6 protons of β -cyclodextrin)



Scheme 2 Structure of *p*-nitrophenol (constructed and optimized by DFT calculations)

p-nitrophenol at around 278 and 224 nm with oscillator strength of 0.2656 and 0.0686, respectively (Table 1). As is known, the calculated oscillator strength can be utilized to aid with comparison of solution phase electronic absorption data [34], and to provide a credible means for the assignment of the observed absorption. As shown in Table 1, three-dimensional contours of the calculated molecular orbitals involved in the transitions were generated and plotted by the Gaussian 03 package. The calculated electrical dipole moment of the transition between molecular orbitals (MOs) 36 and 37, which were the HOMO (highest occupied MO) and LUMO (lowest unoccupied MO) of the guest, was parallel to the X-axis at around 278 nm. The other calculated transition dipole moment between MOs 36 and 38, was determined to be parallel to Y-axis at around 224 nm. The former transition dipole moment in *p*-nitrophenol was almost in the plane of benzene ring and parallel to its X-axis by our TD-DFT calculations. When subject to the Harata and Kodaka's rule, ICD signal at around 278 nm should be positive and

Table 1 Calculated and experimental transition absorption of *p*-nitrophenol

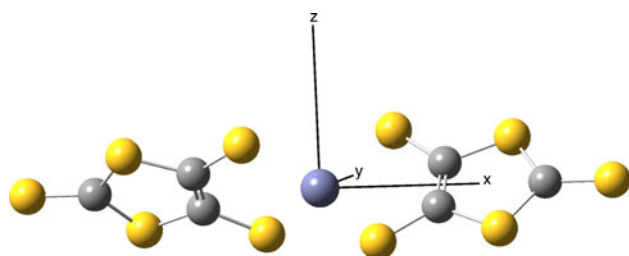
Transition	Calculated absorption (nm)	Experimental absorption (nm)	Transition dipole moment (D) ^a	Oscillator strength ^b	DFT MO contour plots involved in the transition
MO 36 ↓ MO 37	278	329	(1.5586, -0.0384, 0.0000)	0.2656	
MO 36 ↓ MO 38	224	227	(-0.0983, -0.7040, -0.0001)	0.0686	

^a The Cartesian axes are illustrated in Scheme 2, and the three digitals are vectors of the transition dipole moment on X, Y and Z axes respectively. ^b Oscillator strength was predicted by TD-DFT calculations at the optimized geometry

that at 227 nm be negative if *p*-nitrophenol was included into β -cyclodextrin cavity with an X-axial alignment. It turned out to coincide well with the results from literature [35]. Therefore, the transitions at around 278 and 224 nm by our calculations were ascribed to the experimental ones [35] at around 329 and 227 nm, respectively.

As our TD-DFT calculations seemed accessible in prediction of the electric transitions with a pretty goodness-of-fit, we then switched to the assignments of UV and ICD signals of inclusion complex $[\text{Zn}(\text{dmit})_2]^{2-}$ @cyclodextrins. As shown in Scheme 3, the structure of $[\text{Zn}(\text{dmit})_2]^{2-}$ was optimized by our DFT calculations, which was consistent with both the crystal data and the quantum chemistry results [36, 37].

According to our TD-DFT calculations (Table 2), transition 1, with oscillator strength 0.2108, reflected the most intensive absorption which took place between HOMOs and LUMOs of $[\text{Zn}(\text{dmit})_2]^{2-}$. As seen from Table 2, MOs 113 (114) indicated the highest electron density on the sulfur atom while MOs 115 (116) mimicked a π^* anti-bonding orbital. Therefore, transition 1 at around 592 nm was ascribed to the $p \rightarrow \pi^*$ transition of $[\text{Zn}(\text{dmit})_2]^{2-}$ and nearly perpendicular to C=C double bonds. Our result coincided well with that based on the CIS calculations [38], which assigned the transition as p (S) $\rightarrow \pi^*$ (C=S).

**Scheme 3** Structure of $[\text{Zn}(\text{dmit})_2]^{2-}$ (constructed and optimized by DFT calculations)

Transition 2, occurred between MOs 111 (112) and MOs 115 (116), was predicted to have maximum absorption at around 340 nm, and the direction of this transition dipole moment was perpendicular to C=C double bond. Transitions 1 and 2 were somehow overlapped with each other and accounted for the observed broad absorption at around 468 nm for free $[\text{Zn}(\text{dmit})_2]^{2-}$ (UV signals in Figs. 1, 4, 5, 7). Although sheltered by transition 1 in electronic spectra, transition 2 was still recordable (ICD signals in Figs. 1, 4, 5, and 7). The ICD band at around 400 nm most likely reflected the individual dipole moment of transition 2. The other transitions (degenerate transitions 3 and 4, 5 and 6 in Table 2) were predicted as well at around 321 and 304 nm respectively. Our calculations displayed the directions of these transition dipole moments to be perpendicular to the X-axis. They most likely reflected the observed absorptions at around 304 and 276 nm for un-included $[\text{Zn}(\text{dmit})_2]^{2-}$. Since our DFT calculations are based on the highly negatively charged species ($[\text{Zn}(\text{dmit})_2]^{2-}$) in the gas phase, the analyses of our theoretical results have rather a qualitative character. More details are presented in the supplementary material.

It is well known that the Harata and Kodaka's rule presents good accessibility in ICD interpretations of the $\pi \rightarrow \pi^*$ relevant transitions in aromatic chromophores [39, 40] or the $n \rightarrow \pi^*$ relevant transitions in diazirines and azoalkanes systems [41–43], which have been studied in detail. However, whether this theory is applicable in our cases remains unknown, taking into consideration the $p \rightarrow \pi^*$ transition of a transition metal coordination anion $[\text{Zn}(\text{dmit})_2]^{2-}$. And this is the first example to incorporate TD-DFT method into the elucidation of ICD spectra of cyclodextrin inclusion complexes.

The dimension of $[\text{Zn}(\text{dmit})_2]^{2-}$ was illustrated in Scheme 4. Keeping in mind that α -cyclodextrin has a 4.7 Å inner diameter and a 7.9 Å height [5–7], it could merely

Table 2 Calculated and experimental transition absorption of $[\text{Zn}(\text{dmit})_2]^{2-}$

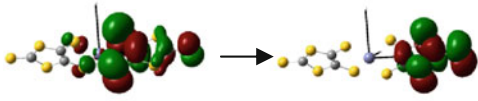
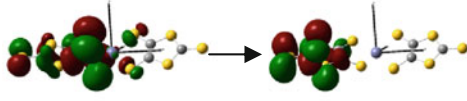
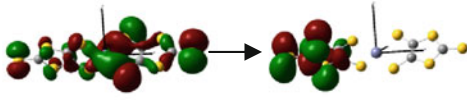


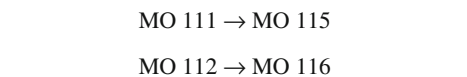
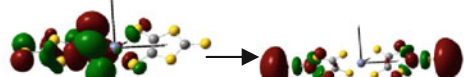

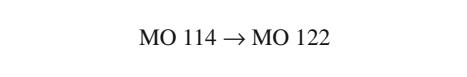

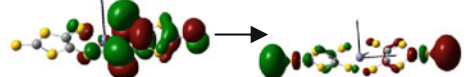

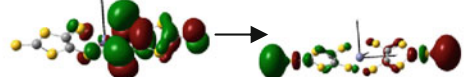
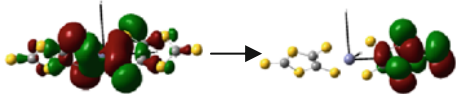
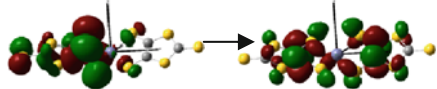
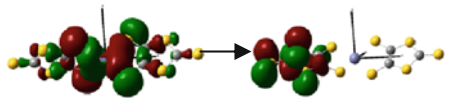

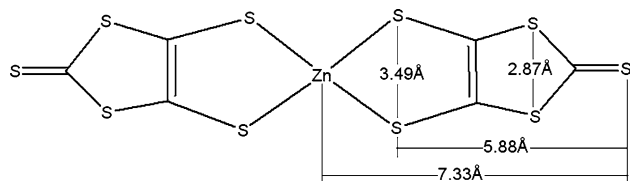
Transition	Calculated absorption (nm)	Experimental absorption (nm)	Transition dipole moment (D) ^a	Oscillator strength ^b	DFT MO and their contour plots involved in the transition
1	592	468 ^c	(-2.0274, -0.0006, -0.0002)	0.2108	 MO 113 → MO 115
		518 ^d			 MO 114 → MO 116
		468 ^e			 MO 111 → MO 116
		514 ^f			 MO 112 → MO 115
2	340	484 ^g	(-0.8760, -0.0004, -0.0001)	0.0685	 MO 111 → MO 116
					 MO 111 → MO 115
					 MO 112 → MO 116
3	321	304 ^c	(-0.0008, 0.2294, 0.2439)	0.0106	 MO 114 → MO 121
		312 ^d			 MO 114 → MO 122
		304 ^e			 MO 113 → MO 121
		322 ^f			 MO 113 → MO 122
4	321	307 ^g	(-0.0008, 0.2438, -0.2294)	0.0106	 MO 113 → MO 121
					 MO 113 → MO 122

Table 2 continued

Transition	Calculated absorption (nm)	Experimental absorption (nm)	Transition dipole moment (D) ^a	Oscillator strength ^b	DFT MO and their contour plots involved in the transition
5	304	276 ^c	(-0.0016, 0.2502, -0.2335)	0.0117	
		276 ^d			MO 104 → MO 115
		272 ^e			
		272 ^f			MO 114 → MO 123
		271 ^g			
6	304		(-0.0056, -0.2317, -0.2476)	0.0117	MO 104 → MO 116
					
					MO 113 → MO 123

^a The Cartesian axes are illustrated in Scheme 3, and the three digitals are vectors of the transition dipole moment on X, Y and Z axes respectively. ^b Oscillator strength was predicted by TD-DFT calculations at the optimized geometry. ^c Absorption maximum of un-included $[\text{Zn}(\text{dmit})_2]^{2-}$. ^d Absorption maximum of $[\text{Zn}(\text{dmit})_2]^{2-}$ in inclusion complex $[\text{Zn}(\text{dmit})_2]^{2-}$ @ β -cyclodextrin. ^e Absorption maximum of $[\text{Zn}(\text{dmit})_2]^{2-}$ in inclusion complex $[\text{Zn}(\text{dmit})_2]^{2-}$ @ α -cyclodextrin. ^f Absorption maximum of $[\text{Zn}(\text{dmit})_2]^{2-}$ in inclusion complex $[\text{Zn}(\text{dmit})_2]^{2-}$ @HP- β -cyclodextrin. ^g Absorption maximum of $[\text{Zn}(\text{dmit})_2]^{2-}$ in inclusion complex $[\text{Zn}(\text{dmit})_2]^{2-}$ @ γ -cyclodextrin

include the guest anion partially. Therefore, the inclusion complexation between $[\text{Zn}(\text{dmit})_2]^{2-}$ and α -cyclodextrin was fairly weak. That's why the ICD signal saturation didn't take place during the α -cyclodextrin titration process (Fig. 4) as it did happen in the cases of $[\text{Zn}(\text{dmit})_2]^{2-}$ @ β -cyclodextrin (Fig. 1), $[\text{Zn}(\text{dmit})_2]^{2-}$ @HP- β -cyclodextrin (Fig. 5), and $[\text{Zn}(\text{dmit})_2]^{2-}$ @ γ -cyclodextrin (Fig. 7). So, the stoichiometry and inclusion constant of inclusion



Scheme 4 Illustration of the dimension of $[\text{Zn}(\text{dmit})_2]^{2-}$ (based on DFT calculations)

complex $[\text{Zn}(\text{dmit})_2]^{2-}$ @ α -cyclodextrin were not computable (vide supra). As β -cyclodextrin has the same height as that of α -cyclodextrin, the 1:2 guest-to-host inclusion ratio (Figs. 2, 11) was reasonable when taking into account the spatial complementarity between $[\text{Zn}(\text{dmit})_2]^{2-}$ anion and the host. However, HP- β -cyclodextrin has about 5 hydroxyl groups randomly substituted by hydroxypropyl groups per molecule of β -cyclodextrin. Due to the formation of hydrogen bonding networks between hydroxyl groups of the side chains and the glucose units, the 2-hydroxypropyl side groups located at the O-2 positions of HP- β -cyclodextrin result in a more "spread out" but dynamically more restricted molecular configuration. It widens cavity entrance at the secondary rim of β -cyclodextrin, and so enhanced the encapsulation capability of HP- β -cyclodextrin [44, 45]. Therefore, more compact and complicated inclusion patterns rather than the 1:2 ratio of guest-to-host

stoichiometry was discovered in inclusion complex $[\text{Zn}(\text{dmit})_2]^{2-}$ @HP- β -cyclodextrin (Fig. 6). Owing to its big inner size (7.5 Å diameter), γ -cyclodextrin couldn't perform such a complementary fitness with the guest that it is found to prefer a 1:1 inclusion model in solution.

Anyway, inclusion complex $[\text{Zn}(\text{dmit})_2]^{2-}$ @ α -cyclodextrin set a good starting point to analyze the above-mentioned ICD signals. Taking into account the dimension of the bar-like guest anion $[\text{Zn}(\text{dmit})_2]^{2-}$, all the cyclodextrins hosts can only have unique co-conformation in the inclusion complexes, which is defined as X-axis alignment (Scheme 3). Therefore, the dipole moment of transition 1 (Table 2) was located outside and penetrated into the α -cyclodextrin cavity according to our DFT calculations, as its magnitude or oscillator strength was intensive. When subject to the Harata and Kodaka's rule, transition 1 was supposed to produce positive ICD signals since it was parallel to the symmetric axis of the host. This hypothesis turned out to be true as the experimental data (ICD signals at around 470–520 nm in Figs. 1, 4, 5, 7) agreed very well with our DFT results. As the oscillator strength of transition 2 (Table 2) was calculated to be weak, the relevant electrical dipole moment was not so intensive as to penetrate into the α -cyclodextrin cavity. So, it is outside the host cavity and parallel to the symmetric axis of α -cyclodextrin. And consequently, transition 2 gave rise to the negative ICD signal at around 395 nm (Fig. 4).

It is known that β - and γ -cyclodextrins have bigger inner size than α -cyclodextrin does (6.0 and 7.5 Å diameter, respectively), therefore these two hosts could perform much deeper inclusion modes. The electrical dipole moment of transition 2 might then have the opportunity to be included inside the hosts' cavities, as the hosts seemed mobile along X-axis of the guest in the inclusion complexes. This assumption could explain the positive ICD signals at around 400 and 410 nm (Figs. 1, 5). The faint ICD trough at around 400 nm in Fig. 7 probably was ascribed to the flexible alignment of inclusion complex $[\text{Zn}(\text{dmit})_2]^{2-}$ @ γ -cyclodextrin in solution.

The degenerate transitions 3 and 4 (Table 2) were calculated to produce electrical dipole moments in the YZ-plane of $[\text{Zn}(\text{dmit})_2]^{2-}$ anion (Scheme 3). Most likely, they were located outside the α -cyclodextrin cavity and perpendicular to the symmetric axis of the host. So, transitions 3 and 4 should generate positive ICD signals if subject to the Harata and Kodaka's rule. The experimental data (ICD bands at around 300–320 nm in Figs. 1, 4, 5, 7) showed that this assumption was applicable in all the examined inclusion complexes.

All the inclusion complexes investigated showed evident ICD troughs at around 270 nm, which was assigned to the transitions 5 and 6 (Table 2). These two transitions were calculated to be in the YZ-plane of $[\text{Zn}(\text{dmit})_2]^{2-}$

anion as well. Based on the experimental data, our DFT prediction didn't work any longer. This could be either the un-accessibility of our DFT calculations in these transitions, or the un-accessibility of the well-known Harata and Kodaka's rule in our case. Taking into consideration the MO contour plots involved in these two transitions, the metal atom was discovered to be involved in. The further exploration and elucidation of these two transitions are still in process in our lab.

Conclusion

In summary, the inclusion complexes of $[\text{Zn}(\text{dmit})_2]^{2-}$ anion with different cyclodextrins hosts were investigated by UV, ICD, $^1\text{H-NMR}$ spectra and DFT calculations in this paper. Due to the spatial complementarities between the guest and the hosts, different inclusion ratios were observed in the inclusion complexes. And the inclusion constants were computed as well based on the experimental data. The results showed that β -, HP- β - and γ -cyclodextrins exhibited strong interactions with the guest, while α -cyclodextrin could merely include $[\text{Zn}(\text{dmit})_2]^{2-}$ anion partially. When in elucidation of the ICD activities of the inclusion complexes, TD-DFT quantum chemistry methods were incorporated in combination with the well-known Harata and Kodaka's rule. The $p \rightarrow \pi^*$ transition of $[\text{Zn}(\text{dmit})_2]^{2-}$ chromophore (at around 468 nm) was calculated to generate an electrical dipole moment, which was located outside but penetrated into the hosts cavities along their symmetrical axes in the inclusion complexes. Our spectroscopic data proved that the $p \rightarrow \pi^*$ transition of $[\text{Zn}(\text{dmit})_2]^{2-}$ chromophore was able to subject to the Harata and Kodaka's rule, which used to be applicable only in the $\pi-\pi^*$ transitions of aromatic chromophores or the $n-\pi^*$ transitions of diazirines and azoalkanes systems. But in the case of other transitions (at around 270 nm), where the molecular orbitals of zinc atom were involved, the DFT calculations was contradictive with the experimental data if still under the Harata and Kodaka's rule.

Acknowledgments We thank the National Nature Science Foundation of China (No. 20771056, 20721002), the National Basic Research Program of China (2010CB923402), Jiangsu Science & Technology Department (BK2008266), and the Center of Analysis and Determining of Nanjing University for financial supports.

References

1. Harata, K., Uedaira, H.: The circular dichroism spectra of the β -cyclodextrin complex with naphthalene derivatives. *Bull. Chem. Soc. Jpn.* **48**, 375–378 (1975)
2. Kodaka, M.: A general rule for circular dichroism induced by a chiral macrocycle. *J. Am. Chem. Soc.* **115**, 3702–3705 (1993)

3. Saenger, W.: Cyclodextrin inclusion compounds in research and industry. *Angew. Chem. Int. Ed.* **19**, 344–362 (1980)
4. Wenz, G.: Cyclodextrin as building blocks for supramolecular structure and functional units. *Angew. Chem. Int. Ed.* **33**, 803–822 (1994)
5. Szejtli, J. Cyclodextrins and their inclusion complexes, Akadémiai Kiadó, Budapest (1982)
6. Bender, M.L., Komiyama, M.: *Cyclodextrin Chemistry*. Springer, Berlin (1978)
7. D'Souza, V.T., Lipkowitz, K.B.: Cyclodextrins: introduction. *Chem. Rev.* **98**, 1741–1742 (1998)
8. Matsui, Y., Yokoi, T., Mochida, K.: Catalytic properties of a copper(II) complex with a modified cyclodextrin. *Chem. Lett.* **10**, 1037–1040 (1976)
9. Breslow, R., Doherty, J.B., Guillot, G., Lipsey, C.: β -Cyclodextrinylbisimidazole, a model for ribonuclease. *J. Am. Chem. Soc.* **100**, 3227–3229 (1978)
10. D'Souza, V.T., Bender, M.L.: Miniature organic models of enzymes. *Acc. Chem. Res.* **20**, 146–152 (1987)
11. Rekharsky, M.V., Inoue, Y.: Complexation thermodynamics of cyclodextrin. *Chem. Rev.* **98**, 1875–1917 (1998)
12. Connors, K.A.: The stability of cyclodextrin complexes in solution. *Chem. Rev.* **97**, 1325–1357 (1997)
13. Lu, Z.D., Lu, C.S., Meng, Q.J.: An inclusion complex of β -cyclodextrin with mnt anion (mnt = maleonitriledithiolate) studied by induced circular dichroism. *J. Incl. Phenom. Macrocycl. Chem.* **61**, 101–106 (2008)
14. Mieusset, J.L., Krois, D., Pacar, M., Brecker, L., Giester, G., Brinker, U.H.: Supramolecular recognition and structural elucidation of inclusion complexes of an achiral carbene precursor in β - and permethylated β -cyclodextrin. *Org. Lett.* **6**, 1967–1970 (2004)
15. Bakirci, H., Zhang, X.Y., Nau, W.M.: Induced circular dichroism and structural assignment of the cyclodextrin inclusion complexes of bicyclic azo-alkanes. *J. Org. Chem.* **70**, 39–46 (2005)
16. Peter, W., Vladimir, B.A., Udo, H.B.: Solvent- and temperature-tuned orientation of ferrocenyl azide inside β -cyclodextrin. *J. Org. Chem.* **71**, 3274–3277 (2006)
17. Cassoux, P., Valade, L., Kobayashi, H., Kobayashi, A., Clark, R.A., Underhill, A.E.: Molecular metals and superconductors derived from metal complexes of 1, 3-dithiol-2-thione-4, 5-dithiolate (dmit). *Coord. Chem. Rev.* **110**, 115–160 (1991)
18. Dai, J., Bian, G.Q., Wang, X., Xu, Q.F., Zhou, M.Y., Munakata, M., Maekawa, M., Tong, M.H., Sun, Z.R., Zeng, H.P.J.: A new method to synthesize unsymmetrical dithiolenic metal complexes of 1, 3-dithiole-2-thione-4, 5-dithiolate for third-order nonlinear optical applications. *J. Am. Chem. Soc.* **122**, 11007–11008 (2000)
19. Cassoux, P.: Molecular (super)conductors derived from bis-dithiolate metal complexes. *Coord. Chem. Rev.* **185**(186), 213–232 (1999)
20. Errami, A., Bowlas, C.J., Menou, F., Faulmann, C., Gangneron, F., Valade, L., Cassoux, P., Lahlil, K., Moradpour, A.: Molecular conducting materials based on $[M(dmit)_2]^{x-}$. *Synth. Met.* **71**, 1895–1896 (1995)
21. Gaussian 03 (Revision B.03), Frisch, M.J.G., Trucks, W., Schlegel, H.B., Scuseria, G.E., Robb, M.A., Cheeseman, J.R., Montgomery Jr., J.A., Vreven, T., Kudin, K.N., Burant, J.C., Millam, J.M., Iyengar, S.S., Tomasi, J., Barone, V. Mennucci, B., Cossi, M., Scalmani, G., Rega, N., Petersson, G.A., Nakatsuji, H., Hada, M., Ehara, M., Toyota, K., Fukuda, R., Hasegawa, J., Ishida, M., Nakajima, T., Honda, Y., Kitao, O., Nakai, H., Klene, M., Li, X., Knox, J.E., Hratchian, H.P., Cross, J.B., Adamo, C., Jaramillo, J., Gomperts, R., Stratmann, R.E., Yazyev, O., Austin, A.J., Cammi, R., Pomelli, C., Ochterski, J.W., Ayala, P.Y., Morokuma, K., Voth, G.A., Salvador, P., Dannenberg, J.J., Zakrzewski, V.G., Dapprich, S., Daniels, A.D., Strain, M.C., Farkas, O., Malick, D.K., Rabuck, A.D., Raghavachari, K., Foresman, J.B., Ortiz, J.V., Cui, Q., Baboul, A.G., Clifford, S., Cioslowski, J., Stefanov, B.B., Liu, G., Liashenko, A., Piskorz, P., Komaromi, I., Martin, R.L., Fox, D.J., Keith, T., Al-Laham, M.A., Peng, C.Y., Nanayakkara, A., Challacombe, M., Gill, P.M.W., Johnson, B., Chen, W., Wong, M.W., Gonzalez, C., Pople, J.A.: Gaussian Inc., Pittsburgh, PA (2003)
22. Briggner, L., Ni, X., Tempesti, F., Wadsö, I.: Microcalorimetric titration of β -cyclodextrin with adamantane-1-carboxylate. *Thermochim Acta* **109**, 139–143 (1986)
23. Eftink, M.R., Andy, M.L., Bystrom, K., Perlmutter, H.D., Kristol, D.S.: Cyclodextrin inclusion complexes: studies of the variation in the size of alicyclic guests. *J. Am. Chem. Soc.* **111**, 6765–6772 (1989)
24. Godínez, L.A., Schwartz, L., Criss, C.M., Kaifer, A.E.: Thermodynamic studies on the cyclodextrin complexation of aromatic and aliphatic guests in water and water-urea mixtures. Experimental evidence for the interaction of urea with arene surfaces. *J. Phys. Chem. B* **101**, 3376–3380 (1997)
25. Hirai, H., Toshima, H., Uenoyam, S.: Inclusion complex formation of γ -cyclodextrin. One host-two guest complexation with water-soluble dyes in ground state. *Bull. Chem. Soc. Jpn.* **58**, 1156–1164 (1985)
26. Fielding, L.: Determination of association constants (K_a) from solution NMR data. *Tetrahedron* **56**, 6151–6170 (2000)
27. Guerrero-Martínez, A., González-Gaitano, G., Vinãs, M.H., Tardajos, G.: Inclusion complexes between β -cyclodextrin and a Gemini surfactant in aqueous solution: an NMR study. *J. Phys. Chem. B* **110**, 13819–13828 (2006)
28. Ali, S.M., Upadhyay, S.K., Maheshwari, A., Koketsu, M.: Complexation of fluvastatin sodium with β -cyclodextrin: NMR spectroscopic study in solution. *J. Incl. Phenom. Macrocycl. Chem.* **55**, 325–328 (2006)
29. Job, P.: Formation and stability of inorganic complexes in solution. *Ann. Chim.* **9**, 113–125 (1925)
30. Stein, T., Kronik, L., Baer, R.: Reliable prediction of charge transfer excitations in molecular complexes using time-dependent density functional theory. *J. Am. Chem. Soc.* **131**, 2818–2820 (2009)
31. Marques, M., Rubio, A., Ullrich, C.A., Burke, K., Nogueira, F., Gross, A.: Time-Dependent Density Functional Theory. Springer, Berlin (2006)
32. Burke, K., Werschnik, J., Gross, E.K.U.: Time-dependent density functional theory: past, present, and future. *J. Chem. Phys.* **123**, 0622061–0622069 (2005)
33. Chelikowsky, J.R., Kronik, L., Vasiliev, I.: Time-dependent density-functional calculations for the optical spectra of molecules, clusters, and nanocrystals. *J. Phys. Condens. Matter.* **15**, 1517–1547 (2003)
34. Waters, T., Wang, X.B., Yang, X., Zhang, L., Richard, A.J., Wang, L.S., Wedd, A.G.: Photoelectron spectroscopy of the doubly-charged anions $[MIVO(mnt)_2]^{2-}$ ($M = Mo, W$; $mnt = S_2C_2(CN)_2^{2-}$): access to the ground and excited states of the $[MVO(mnt)_2]^-$ anion. *J. Am. Chem. Soc.* **126**, 5119–5129 (2004)
35. Shimizu, H., Kaito, A., Hatano, M.: Induced circular dichroism of cyclodextrin complexes with substituted benzenes. *Bull. Chem. Soc. Jpn.* **52**, 2678–2684 (1979)
36. Chohan, Z.H., Howie, R.A., Wardell, J.L., Wilkens, R., Doidge-Harrison, S.M.S.V.: Synthesis of bis[(ferrocenylmethyl)trimethylammonium] [bis(1, 3-dithiole-2-thione-4, 5-dithiolato)zincate] and [bis(1, 3-dithiole-2-one-4, 5-dithiolato)zincate] salts, $[(FeCH_2NMe_3)_2[Zn(dmit)_2]]$ and $[FeCH_2NMe_3)_2[Zn(dmio)_2]]$: crystal structures of $[FeCH_2NMe_3)_2[Zn(dmit)_2]]$ and $[NEt_4)_2[Zn(dmit)_2]]$. *MeOH. Polyhedron* **16**, 2689–2696 (1997)

37. Harrison, W.T.A., Howie, R.A., Wardell, J.L., Wardell, S.M.S.V., Comerlato, N.M., Costa, L.A.S., Silvino, A.C., de Oliveira, A.I., Silva, R.M.: Crystal structures of three [bis(1, 3-dithiole-2-thione-4, 5-dithiolato)zincate]²⁻ salts: [Q]₂[Zn(dmit)₂] (Q = 1, 4-Me₂-pyridinium or NEt₄) and [PPh₄]₂[Zn(dmit)₂] DMSO. Comparison of the dianion packing arrangements in [Q]₂[Zn(dmit)₂]. *Polyhedron* **19**, 821–827 (2000)
38. Ferreira, G.B., Hollauer, E., Comerlato, N., Wardell, J.: An experimental and theoretical study of the electronic spectra of tetraethylammonium [bis(1, 3-dithiole-2-thione-4, 5-dithiolato)zincate(II)], [NEt₄]₂[Zn(dmit)₂], and tetraethylammonium [bis(1, 3-dithiole-2-one-4, 5-dithiolato)zincate(II)], [NEt₄]₂[Zn(dmit)₂]. *Inorg. Chim. Acta* **359**, 1239–1247 (2006)
39. Shimizu, H., Kaito, A., Hatano, M.: Induced circular dichroism of β-cyclodextrin complexes with substituted benzenes. *Bull. Chem. Soc. Jpn.* **52**, 2678–2684 (1979)
40. Shimizu, H., Kaito, A., Hatano, M.: Induced circular dichroism of β-cyclodextrin complexes with o-, m-, and p-disubstituted benzenes. *Bull. Chem. Soc. Jpn.* **54**, 513–519 (1981)
41. Zhang, X., Nau, W.M.: Chromophore alignment in a chiral host provides a sensitive test for the orientation-intensity rule of induced circular dichroism. *Angew. Chem. Int. Ed.* **39**, 544–547 (2000)
42. Mayer, B., Zhang, X., Nau, W.M., Marconi, G.: Co-conformational variability of cyclodextrin complexes studied by induced circular dichroism of azoalkanes. *J. Am. Chem. Soc.* **123**, 5240–5248 (2001)
43. Zhang, X., Gramlich, G., Wang, X., Nau, W.M.: A joint structural, kinetic, and thermodynamic investigation of substituent effects on host-guest complexation of bicyclic azoalkanes by beta-cyclodextrin. *J. Am. Chem. Soc.* **124**, 254–263 (2002)
44. Yong, C.W., Clive, W., William, S.: Structural behaviour of 2-hydroxypropyl-β-cyclodextrin in water: molecular dynamics simulation studies. *Pharm. Res.* **25**, 1092–1099 (2008)
45. Castronuovo, G., Niccoli, M., Varriale, L.: Complexation forces in aqueous solution. Calorimetric studies of the association of 2-hydroxypropyl-β-cyclodextrin with monocarboxylic acids or cycloalkanol. *Tetrahedron* **63**, 7047–7052 (2007)